CHAPTER V

MESOPOROUS SAPO-5 WITH AFI-TYPE PREPARED VIA MICROWAVE RADIATION USING ALUMATRANE AND SILATRANE PRECURSORS

5.1 Abstract

A new class of mesoporous zeotype, SAPO-5, has been prepared using alumatrane and silatrane precursors, containing alkanolamine ligands, via microwave radiation. Triethylamine (TEA) was used as a structure-directing agent. The effects of the amount of silicon, the reaction conditions, viz. aging time, reaction temperature and time were investigated. All samples were characterized using X-ray diffraction (XRD), scanning electron microscopy (SEM), transmission electron microscope (TEM), X-ray fluorescence (XRF), and surface area analyzer. The results showed SAPO-5 zeotype with AFI-type having a hexagonal outer surface morphology, BET surface areas in the range of 270–320 m^2/g, and an average pore diameter of 2–5 nm. The samples contained a classical single crystal of SAPO-5 and 10–100 nm mesoporous matrix nanostructure having AFI structure.

5.2 Introduction

Owing to the benefits obtained from the combination of mesoporous molecular sieves and zeolites [1–3], such as improvement of the mass transfer to and from the active sites to solve the problem of diffusion limitation of micropore, enhancement of the catalytic properties, as compared to conventional zeolites [4-5], mesoporous $AlPO_4$-5 zeotype has recently been studied and synthesized [2,6]. The $AlPO_4$-5 zeotype with AFI-type molecular sieve, having unidimensional 12-membered rings of straight channels, exhibits the property of excellent thermal stability and is widely used in areas of catalysis, separation [7], membranes, sensors, and nonlinear optics [8]. Egleblad *et al.* [2] prepared mesoporous $AlPO_4$-5 with AFI type by introducing a carbon particle template via fluoride route under conventional heating for 3 days. To reduce reaction time and to use a simple route for the synthesis, mesoporous $AlPO_4$-5 (AFI) zeotype has been obtained within 2 h using an

alumatrane precursor containing a bulky group of trialkanoamine ligand via microwave technique [6].

The synthesis of AlPOs, zeolites, and other porous materials under microwave heating has overcome many drawbacks found when using conventional heating, such as fast crystallization [9–12], high phase purity [13, 14], high phase selectivity [15–17], and narrow particle size distribution [18]. However, the $AlPO_4$-5 material composing of AlO_4^- and PO_4^+ tetrahedra link in a neutral framework shows no Bronsted acidity. The introduction of Si atoms to the neutral $AlPO_4$-5 structure generates silicoaluminophosphate, SAPO-5, capable of producing cation exchange properties and inducing Bronsted acid sites into the framework to be further used as acid catalysts since it provides a much stronger interaction with the hydrocarbons [1]. The effect of silica content on the synthesis of microporous SAPO-5 with AFI type has been studied by several groups [19–21]. They showed that Si atoms affected the AFI framework by hindering the crystallization to form plate-like hexagonal crystals [21]. The uses of alumina and silica sources have also been reported to affect the phase purity [19, 22, 23], crystallinity, acidity, and morphology of the products [23, 24]. As reported in literature [1–3], mesoporous zeolite and zeotype, such as BEA, MEL, CHA, MFI, and AFI, have been successfully prepared. However, mesoporous SAPO-5 has not yet been studied. From our previous works of mesoporous $AlPO_4$-5 [6], alumatrane [25], and silatrane [26], SAPO-5 has thus been further studied and synthesized in this work using atrane precursors and TEA as a structure-directing agent under microwave radiation. The effects of chemical compositions and reaction conditions were investigated.

5.3 Experimental

5.3.1 Materials Characterization

Functional groups of materials were followed using FTIR spectrophotometer (Nicolet, NEXUS 670) with a resolution of 4 cm^{-1}. Thermogravimetric analysis (TGA) was carried out using TG-DTA (Pyris Diamond Perkin Elmer) with a heating rate of 10 °C/min in the range of room temperature to 750 °C under nitrogen

atmosphere to determine the thermal stability. BET surface area measurement, pore volume and pore size distribution were measured using nitrogen at 77 K in an Autusorb-1 gas sorption system (Quantasorb JR). Samples were degassed at 250 °C under a reduced pressure prior to each measurement. Total surface area was calculated according to the BET method. Micropore and mesopore volumes were determined by the *t*- and BJH methods (desorption). Product morphology was studied on a JEOL 5200-2AE scanning electron microscope. Chemical composition of the samples was determined by XRF (Philips PW 2400) and SEM (JEOL JSM-5410LV) equipped with energy-dispersive analysis of X-rays (EDAX) microanalysis measurements performed on an Oxford Link Isis instrument. TEM micrographs were recorded on JEOL JEM-2100 for characterizing the pore system of the samples. Calcination was performed on a Carbolite Furnace (CFS 1200) with a heating rate of 1 °C/min. Hydrothermal crystallization by microwave heating technique was carried out on Milestone's Ethos microwave solvent extraction labstation with the frequency of the microwave radiation of 2.45GHz. Crystallinity characterization of samples was conducted on Rigaku X-ray diffractometer with CuKα source in a range of 5° to 60° with a step of 5°/min, using the following equation;

$$\%\text{crystallinity} = (\sum I / \sum I_s)*100$$

where I is the line intensity of the sample and I_s is the line intensity of the standard sample, using the product having the highest crystallinity, as identified by XRD and supported by SEM. The line intensities of the XRD pattern at 2Θ = 7.5, 14.9, 19.8, 21.1, 22.5 and 26.0 degree [27] were employed for these calculations.

5.3.2 Methodology

5.3.2.1 Synthesis of Alumatrane

The preparation of alumatrane followed the work of Opornsawad *et al.* [25]. Aluminium hydroxide (0.1 mole, Sigma Chemical Co.) triisopropanolamine (TIS, 0.125 mole, Aldrich Chemical Co. Inc., USA) and ethylene glycol (EG, 100 ml, J.T. Baker, Inc., Phillipsburg, USA) were added into a 250 ml two-necked round bottom flask. The mixture was homogeneously stirred at room temperature before being

heated to 200 °C under nitrogen in an oil bath for 10 h. Excess EG was removed under vacuum (10^{-2} Torr) at 110 °C to obtain crude product. The crude solid was washed with acetonitrile (Lab-Scan Company Co., Ltd.) and dried under vacuum at room temperature. Dried products were characterized using TGA and FTIR.

FTIR: 3700-3300 cm^{-1} (ν OH), 2750-3000 cm^{-1} (ν CH), 1650 cm^{-1} (ν OH overtone), 1460 cm^{-1} (δ CH), 1078 cm^{-1} (ν Al–O–C) and 500–800 cm^{-1} (ν Al–O). TGA: 33 % char yield which is larger than the theoretical ceramic value of 23.7 %. This may be due to the incomplete combustion which was confirmed by the black color of the char.

5.3.2.2 Synthesis of Silatrane

Silatrane was synthesized using the process identical to the alumatrane synthesis [26] by mixing fume silica (0.1 mole, 99.8% SiO_2, Sigma Chemical Co.), triethanolamine (0.125 mole, Aldrich Chemical Co. Inc., USA) and EG (100 ml) in a 250 ml two-necked round bottom flask. The mixture was heated to the boiling point of EG under nitrogen for 10 h in an oil bath. The rest of EG was removed under vacuum at 110 °C to obtain a brownish white solid, followed by washing with acetronitrile to obtain white powder and dried under vacuum at room temperature before characterization using TGA and FTIR.

FTIR: 3700-3300 cm^{-1} (ν OH), 2800-3000 cm^{-1} (ν CH), 1244–1275 cm^{-1} (ν CN), 1170 –1117 cm^{-1} (ν Si–O), 1093 cm^{-1} (ν Si–O–C), 1073 cm^{-1} (ν CO), 785 and 729 cm^{-1} (Si–O–C), and 579 cm^{-1} (ν N → Si). TGA: 19 % ceramic yield which is close to the theoretical value, 18.5 %.

5.3.2.3 Preparation of SAPO-5 (AFI)-type Zeotype

Alumatrane was mixed with 1M phosphoric acid solution under homogeneous stirring at room temperature. Silatrane was added to the mixture with various mole ratios of SiO_2/Al_2O_3, followed by adding TEA (Fisher Scientific) as a structure-directing agent. The mixture was aged with stirring at various aging time

before being loaded into a Teflon line vessel sealed with a Teflon cap and placed in a microwave oven. The reaction mixture was heated at various temperatures (180 °–200 °C) for various times (0.5–2 h). After reaction, the pH value was 6.5, being nearly the same as the pH value before hydrothermal treatment. The products were filtered, washed, and dried. The as-synthesized products were calcined at 550 °C for 7 h. The amount of SiO_2 content, aging time, and reaction conditions were varied.

5.4 Results and Discussion

In the present work a series of SAPO-5 with AFI-type material was prepared using various reaction conditions and chemical compositions of the atrane precursors under microwave radiation. The XRD patterns of the products correspond well with the structure pattern of AFI-type topology reported in references 20, 21, and 28. The SEM images showed that all synthesized SAPO-5 samples have a well-formed hexagonal outer surface. Demuth *et al.* [19] found that to obtain white powder product of SAPO-5 the samples had to be calcined at 850 °C for at least 24 h. However, in our case the SAPO-5 product using atrane precursors was synthesized at only 550 °C for 7h to remove organic residues.

5.4.1 Effect of aging time

The SEM images shown in Figure 5.1 illustrate SAPO-5 prepared from the reaction gels of Al_2O_3:$2P_2O_5$:$0.2SiO_2$:1.5TEA:$750H_2O$, aged with stirring for various times (4–24 h), and heated at 190 °C for 1 h. To keep the pH value of the synthesis mixture at nearly neutral, the mole ratio of Al_2O_3/P_2O_5 was fixed to 1:2 throughout all conditions. It was found that the smaller and more uniform SAPO-5 crystals were formed at prolonged aging time owing to a higher number of nucleation centers created by agitation of the gel, as discussed by Du and coworkers [29]. Further increasing the aging time to 24 h produced crystals that were still smaller in size, but had lower homogeneity than those aged for 16 h. Moreover, the XRD patterns of the same samples (Figure 5.2) indeed show the pattern of pure SAPO-5 structure without

any impurity, except the sample aged for 24 h (Figure 5.2d) showing a small amount of impurity which was identified as tridymite phase [30] coexisting with the AFI-type structure. The impurity phase was also observed by Chen and coworker when loading a high amount of metal onto the AFI framework of $AlPO_4$-5 [30]. The proper aging time of 16 h was thus selected for further study.

5.4.2 Effect of reaction time

The mixture composition of Al_2O_3:$2P_2O_5$:$0.2SiO_2$:1.5TEA:$750H_2O$, the aging time of 16 h, and the reaction temperature of 190 °C were fixed to investigate the effect of reaction time on the crystallization of SAPO-5. The reaction duration was varied from 0.5 to 2 h. The results in Figure 5.3 show that the sample synthesized for 0.5 h microwave heating time resulted in SAPO-5 crystals mixed with some amorphous phase (Figure 5.3a), implying that there was not enough time for SAPO-5 to be completely formed. On increasing the reaction time to 1 h, SAPO-5 crystals were obtained. As reaction duration was increased to more than 1 h, secondary growth of SAPO-5 crystals started to occur and became non-uniform. Thus, the reaction time of 1 h is chosen to study other effects.

5.4.3 Effect of reaction temperature

The chemical composition of Al_2O_3:$2P_2O_5$:$0.2SiO_2$:1.5TEA:$750H_2O$, the aging time of 16 h, and the reaction time of 1 h were fixed for studying the effect of reaction temperature which has been varied between 180 °C and 200 °C (Figure 5.4 a-c). At the lowest microwave temperature of 180 °C, it seems that the temperature was not high enough for perfect crystals to be formed. Amorphous growth covered the entire SAPO-5 product. This result can be confirmed by the XRD pattern in Figure 5a, showing not only lower intensity, but also a curvature base line, indicating the presence of an amorphous phase. When the temperature was increased to 190 °C, pure and uniform SAPO-5 crystals with a hexagonal plate-like structure (Figure 5.4b, 5.5b) were obtained. However, a reaction temperature of 200 °C does not seem to provide a higher quality of the crystals. In addition to SAPO-5 crystals, small

amounts of tridymite [30], as can be seen in Figure 5.5c, were also obtained. These results are in good agreement with the work done by Demuth *et al.* [19] who obtained pure phase of SAPO-5 at the reaction temperature of 210 °C, and did not obtain SAPO-5 at lower temperatures, 170 °-190 °C. Furthermore, when they increased the reaction temperature to higher than 210 °C, a mixture of the crystals of SAPO-5 and tridymite was obtained. In our case trialkoxylamines generated from both silatrane and alumatrane precursors during the reaction could act as co-directing agents to form pure phase of SAPO-5 at 190 °C, as discussed elsewhere [31]. These results indicate that there is a temperature-time optimum controlling the reaction conditions for the synthesis of a pure phase of SAPO-5 materials.

5.4.4 Effect of silicon content

The mixture composition of Al_2O_3:$2P_2O_5$:$x$$SiO_2$:1.5TEA:$750H_2O$ was used to study the effect of silicon loading into the AFI framework. The amount of SiO_2 was varied from 0 to 1.0 mole ratio of SiO_2 to Al_2O_3. Figure 5.6 illustrates the SEM images of the crystals obtained using various silicon contents. It was found that the sample prepared without silicon in the reactant gel showed a long hexagonal rod-like structure (Figure 5.6a) which is the characteristic of $AlPO_4$-5 with AFI topology [6, 27]. When loading silicon dioxide into the same chemical compositions of gel, it showed that the crystal morphology became a short plate-like hexagon (Figure 5.6 b-f). This result is in agreement with the study of Demuth *et al.* [19] who also indicated that the incorporation of Si atoms into AFI-type framework influenced the crystal growth in the *c*-axis. Moreover, at higher silicon contents loaded in the reactant gels, > 0.2, amorphous impurity occurred along with the obtained hexagonal plate-like crystals, as confirmed by calculating the % crystallinity summarized in Table 5.1 and the XRD spectra in Figure 5.7. It can be seen clearly from Table 5.1 that the higher amount of silicon loaded beyond 0.2, the lower crystallinity of SAPO-5 materials was obtained (Table 5.1). It was also reported by Akolekar [32]. He studied the effect of the silicon amount (0-0.224 mole ratio of SiO_2 to Al_2O_3) in SAPO-5 crystals using pseudo-boehmite and Kieselgel 500 as Al_2O_3 and SiO_2 sources, respectively, and found that the crystallinity of SAPO-5 decreased with the silicon amount. From

Figure 5.7 showing only the SAPO-5 phase, it can be concluded that highly crystalline SAPO-5 could be synthesized with the SiO_2 to Al_2O_3 mole ratio up to 0.8 in the reactant gels. The addition of silicon atoms into the AFI framework not only generates Bronsted acid sites, as described earlier, but also controls the morphology of the crystals. It is worth noting that for the long hexagonal rod-like crystals which AFI grew preferentially in the *c*-direction (Figure 5.6a), the relative diffraction intensity of the *h k l* planes of {0 0 2} is much lower (Figure 5.7a) while in the case of the short hexagonal plate-like crystal of AFI-type (Figure 5.6 b-e), the intensity of the same plane is very high (Figure 5.7 b-e), as compared to the other planes, {1 0 0}, {2 1 0} and {1 0 2}. This result is in agreement with previous results studied by Jhung *et al.* [21, 33], who synthesized microporous AFI crystals, both $AlPO_4$-5 and SAPO-5, and found that with plate-like hexagonal crystals in the case of Si loading into AFI framework the relative intensity of {0 0 2} diffraction to {1 0 0}, {2 1 0} and {1 0 2} was also high.

The XRF and EDX/SEM results in Figure 5.8 show the amounts of the silicon in the SAPO-5 products compared to those loaded in the gels. It exhibited that the amount of the silicon in the products was lower than the actual loading, indicating not all Si present in the synthesis gel was incorporated into the synthesis product.

The existence of the mesopore SAPO-5 prepared using the chemical composition of Al_2O_3:$2P_2O_5$:$0.2SiO_2$:1.5TEA:$750H_2O$ at the reaction temperature of 190 °C for 1 h was confirmed using TEM. It was found that the obtaining hexagonal crystals (Figure 5.9a) showed characteristics of AFI structure containing one dimensional channel while mesoporous nanostructure (not the hexagonal crystal region) in Figure 5.9b was also AFI type, as confirmed by SAED in Figure 5.9c, also showing hexagonal characteristics. As a result, the synthesized AFI products contained both classical single crystals and 10-100 nm mesoporous matrix nanostructure of SAPO-5.

5.4.5 Nitrogen physisorption

The nitrogen adsorption-desorption isotherms and pore size distribution of the SAPO-5 materials obtained using the chemical composition of Al_2O_3:$2P_2O_5$:$0.2SiO_2$: 1.5TEA:$750H_2O$ are shown in Figure 5.10. The obtained isotherms of type IV imply that these materials are mesoporous, similar to those found in other mesoporous zeolites [2, 5]. It is seen that all materials contain mesopore with an average pore diameter of about 2–5 nm. The BET surface areas, micropore and mesopore volumes for samples prepared using different silicon contents are summarized in Table 5.2. All the synthesized SAPO-5 molecular sieves have a BET surface area in the range of 270–320 m^2g^{-1}. The physisorptions of the other samples also gave similar results, corresponding to mesoporous materials (not shown), exhibiting that SAPO-5 prepared from an atrane route under microwave radiation resulted in the presence of mesoporous structure. These profiles result from TIS and triethanolamine molecules generated from the hydrolysis of alumatrane and silatrane during the SAPO-5 synthesis to form AFI framework, respectively, because both triethanolamine and TIS could be used as co-directing agents in the synthesis mixture to stabilize the structure formation of SAPO-5 with AFI topology, as reported in previous works [6, 34, 35]. Generally, alkanoamines; e.g. triethanolamine and TIS, were used as a stabilizing and buffering or complexing agent in the synthesis of porous materials. It may be concluded that the mixture of TEA structure-directing agent, triethanolamine, and TIS molecules generated mesoporous SAPO-5 zeotype.

5.5 Conclusions

Mesoporous SAPO-5 has been successfully synthesized using alumatrane and silatrane precursors, as alumina and silica source, respectively, via microwave heating technique. The reaction conditions, viz. aging time, microwave temperature and time have influence on the SAPO-5 formation. The amount of the SiO_2 content up to 0.8 mole ratio of SiO_2 to Al_2O_3 could be loaded to the reaction gels to form highly crystalline SAPO-5. All samples contained a classical single crystal of SAPO-5 and 10-100 nm mesoporous matrix nanostructure having AFI structure.

5.6 Acknowledgements

This research work is financially supported by the Postgraduate Education and Research Program in Petroleum and Petrochemical Technology (ADB) Fund, the Ratchadapisake Sompote Fund, Chulalongkorn University, and the Development and Promotion of Science and Technology Thailand Project (DPST).

5.7 References

1. C.J.H. Jacobsen, C. Madsen, J. Houzvicka, I. Schmidt, A. Carlsson, J. Am. Chem. Soc. 122 (2000) 7116.
2. K. Egeblad, M. Kustova, S.K. Klitgaard, K. Zhu, C.H. Christensen, Micropor. Mesopor. Mater. 101 (2007) 214.
3. V. Naydenov, L. Tosheva, O.N. Antzutkin, J. Sterte, Micropor. Mesopor. Mater. 78 (2005) 181.
4. C.H. Christensen, K. Johannsen, I. Schmidt, C.H. Christensen, J. Am. Chem. Soc. 125 (2003) 13370.
5. F.S. Xiao, L. Wang, C. Yin, K. Lin, Y. Di, J. Li, R. Xu, D.S. Su, R. Schlogl, T. Yokoi, T. Tatsumi, Angew. Chem. Int. Ed. 45 (2006) 3090.
6. K. Utchariyajit, S. Wongkasemjit, Micropor. Mesopor. Mater., 114 (2008) 175.
7. S.T. Wilson, B.M. Lok, C.A. Messina, T.R. Cannan, E.M. Flanigen, J. Am.Chem. Soc. 104 (1982) 1146.
8. J. Caro, G. Finger, J. Kornatowski, J.R. Mendau, L. Werner, B. Zibrowius, Adv. Mater. 4 (1992) 273.
9. S. Komarneni, R. Roy, Q. H. Li, Mat. Res. Bull. 27 (1992) 1393.
10. S. Komarneni, Q.H. Li, R. Roy, J. Mat. Chem. 4 (1994) 1903.
11. S. Komarneni, Q. H. Li, R. Roy, J. Mat. Res. 11 (1996) 1866.
12. S.C. Laha, G. Kamalakar, R. Glaser, Micropor. Mesopor. Mater. 90 (2006) 45.
13. M. Park, S. Komarneni, Micropor. Mesopor. Mater. 20 (1998) 39.
14. S. Mintova, S. Mo, T. Bein, Chem. Mater. 10 (1998) 4030.
15. S.H. Jhung, J.S. Chang, J.H. Lee, J.S. Hwang, S.E. Park, J.S. Chang, Micropor. Mesopor. Mater. 64 (2003) 33.
16. J.W. Yoon, S.H. Jhung, Y.H. Kim, S.E. Park, J.S. Chang, Bull. Korean Chem. Soc. 26 (2005) 558.

17. S.H. Jhung, J.H. Lee, J.W. Yoon, J.S. Hwang, S.E. Park, J.S. Chang, Micropor. Mesopor. Mater. 80 (2005) 147.
18. T. Kodaira, K. Miyazawa, T. Ikeda, Y. Kiyozumi, Micropor. Mesopor. Mater. 29 (1999) 329.
19. D. Demuth, G.D. Stucky, K.K. Unger, F. Schuth, Micropor. Mater. 3, (1995) 473.
20. R. Roldan, M.S. Sanchez, G. Sankar, F.J.R. Salguero, C.J. Sanchidrian, Micropor. Mesopor. Mater. 99 (2007) 288.
21. S.H. Jhung, J.S. Chang, D.S. Kim, S.E. Park Micropor. Mesopor. Mater. 71 (2004) 135.
22. S.K. Saha, S.B. Waghmode, H. Maekawa, K. Komura, Y. Kobuta, Y. Sugi, Y. Oumi, T. Sano, Micropor. Mesopor. Mater. 81 (2005) 289.
23. N. Kumar, J.I. Villegas, T. Salmi, D.Y. Murzin, T. Heikkila, Catal. Today. 100, (2005) 355.
24. A.K. Sinha, S. Sainkar, S. Sivasanker, Micropor. Mesopor. Mater. 31 (1999) 321.
25. Y. Opornsawad, B. Ksapabutr, S. Wongkasemjit, R.M. Laine, J. Eur. Polym. 37, (2001) 1877.
26. P. Piboonchaisit, S. Wongkasemjit, R. Lanine, ScienceAsia. 25 (1999) 113.
27. Y. Wan, C.D. Williams, C.V.A. Duke, J.J. Cox, J. Mater. Chem. 10 (2000) 2857.
28. L. Wang, C. Gua, S. Yan, X. Huang, Q. Li, Micropor. Mesopor. Mater. 64 (2003) 63.
29. H. Du, M. Fang, W. Xu, X. Meng, W. Pang, J. Mater. Chem. 7 (1997) 551.
30. C.M. Chen, J.M. Jehng, Catal. Lette. 93 (2004) 213.
31. P. Phiriyawirut, R. Magaraphan, A. Jamieson and S. Wongkasemjit, Mesopor. Micropor. Mater. 64 (2003) 83.
32. D.B. Akolekar, J. Catal. 149 (1994) 1.
33. S.H. Jhung, J.S. Chang, Y.K. Hwang, J. Mater. Chem. 14 (2004) 280.
34. E.N. Coker, J.C. Jansen, Mol. Sieves 1 (1998) 121.
35. S.T. Wilson, B.M. Lok, E.M. Flanigen, US Pat. 4 310 440 (1982).

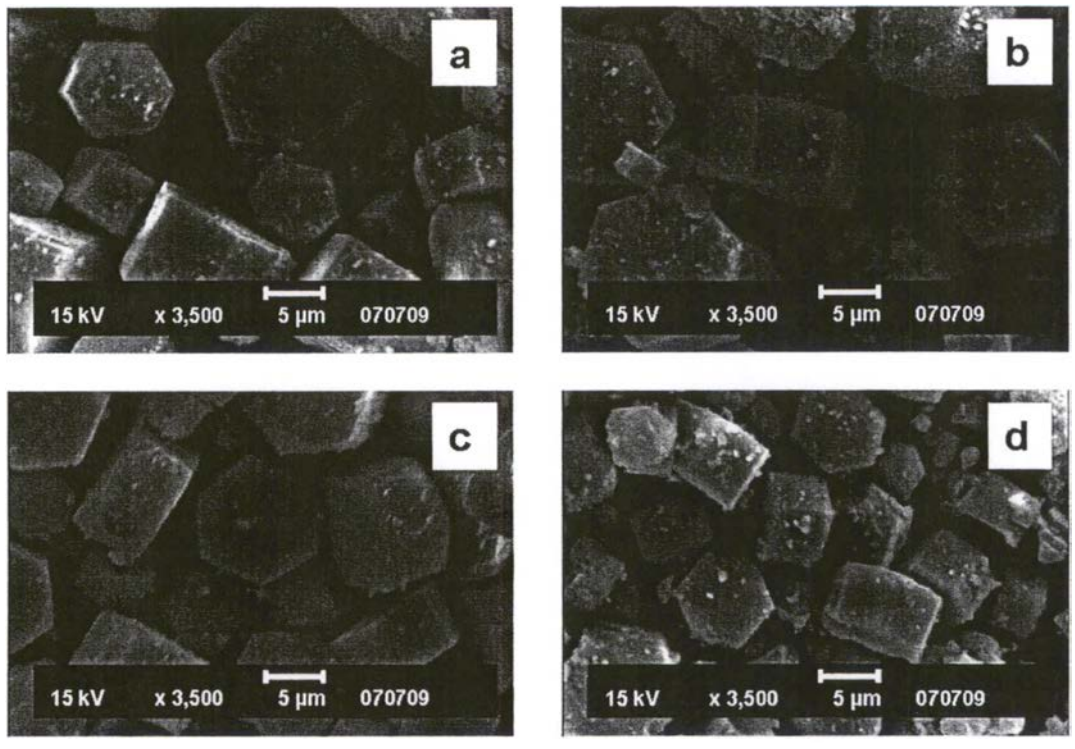

Figure 5.1 SEM images of SAPO-5 prepared from the mixture of Al_2O_3:$2P_2O_5$: $0.2SiO_2$:1.5TEA:$750H_2O$, heated at 190 °C for 1h, and aged for (a) 4, (b) 8, (c) 16, and (d) 24 h.

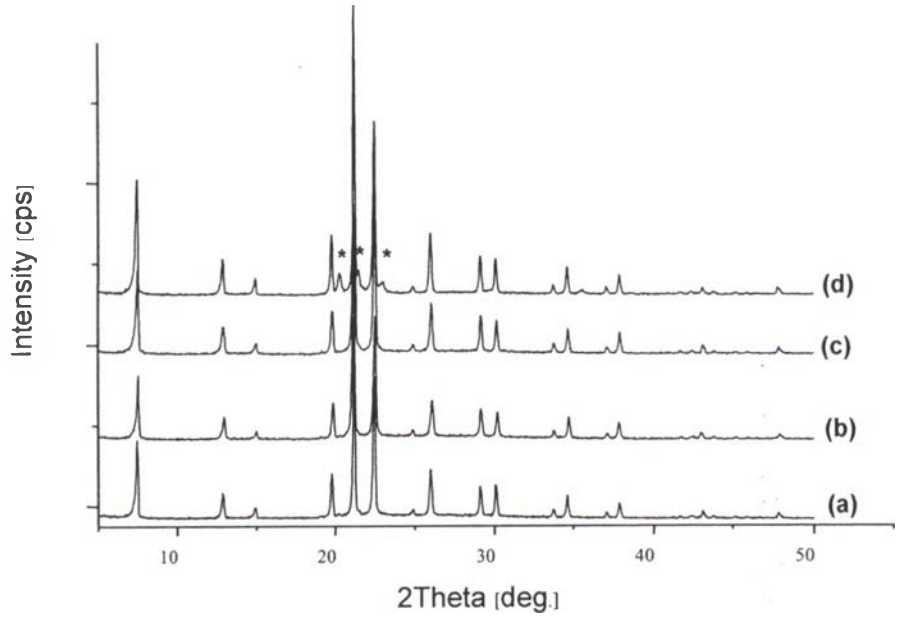

Figure 5.2 XRD patterns of SAPO-5 synthesized from the mixture of Al_2O_3:$2P_2O_5$: $0.2SiO_2$:1.5TEA:$750H_2O$ at 190 °C 1h and aged for (a) 4, (b) 8, (c) 16, and (d) 24 h. (Note: * refers to tridymite phase)

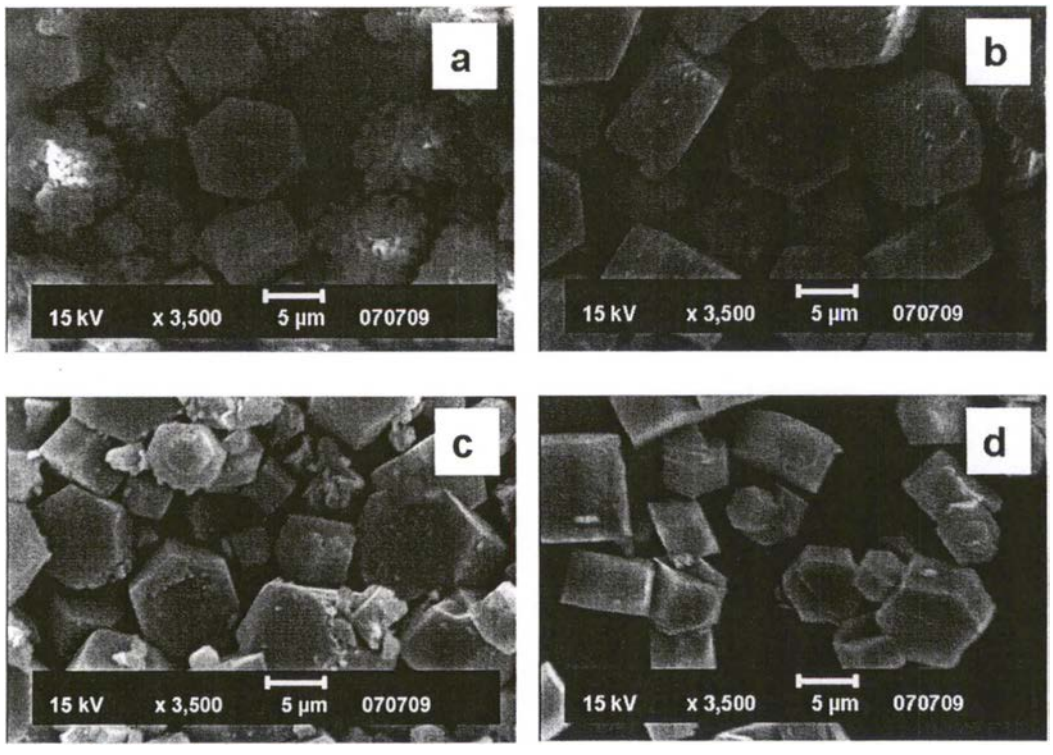

Figure 5.3 SEM images of SAPO-5 prepared from the mixture of Al_2O_3:$2P_2O_5$: $0.2SiO_2$:1.5TEA:$750H_2O$ at 190 °C microwave heating temperature for (a) 0.5, (b) 1, (c) 1.5, and (d) 2 h.

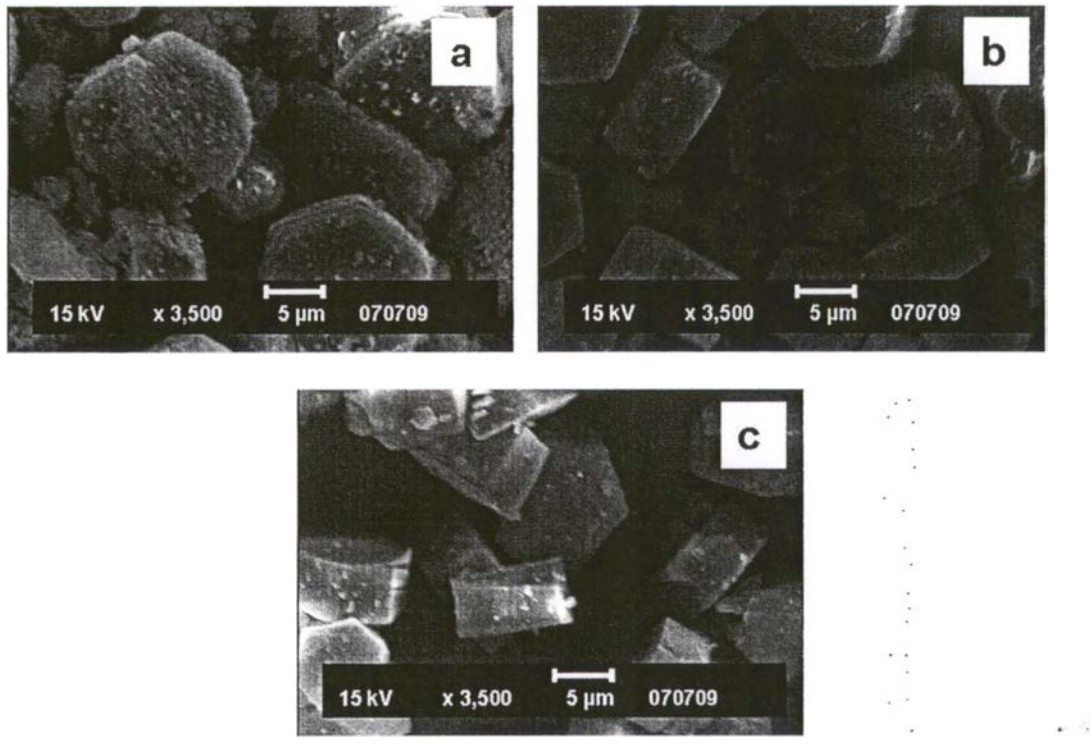

Figure 5.4 SEM images of SAPO-5 obtained from the mixture of Al_2O_3:$2P_2O_5$: $0.2SiO_2$:1.5TEA:$750H_2O$ for 1h reaction time at reaction temperature of (a) 180 °C, (b) 190 °C, and (c) 200 °C.

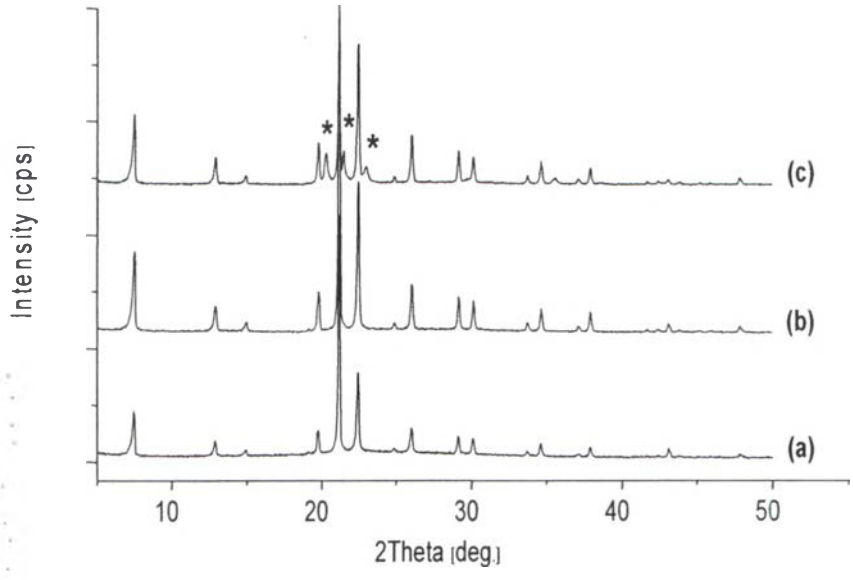

Figure 5.5 XRD patterns of SAPO-5 synthesized from the mixture of Al_2O_3:$2P_2O_5$: $0.2SiO_2$:1.5TEA:$750H_2O$ for 1h reaction time at reaction temperature of (a) 180 °C, (b) 190 °C, and (c) 200 °C. (Note: * refers to tridymite phase)

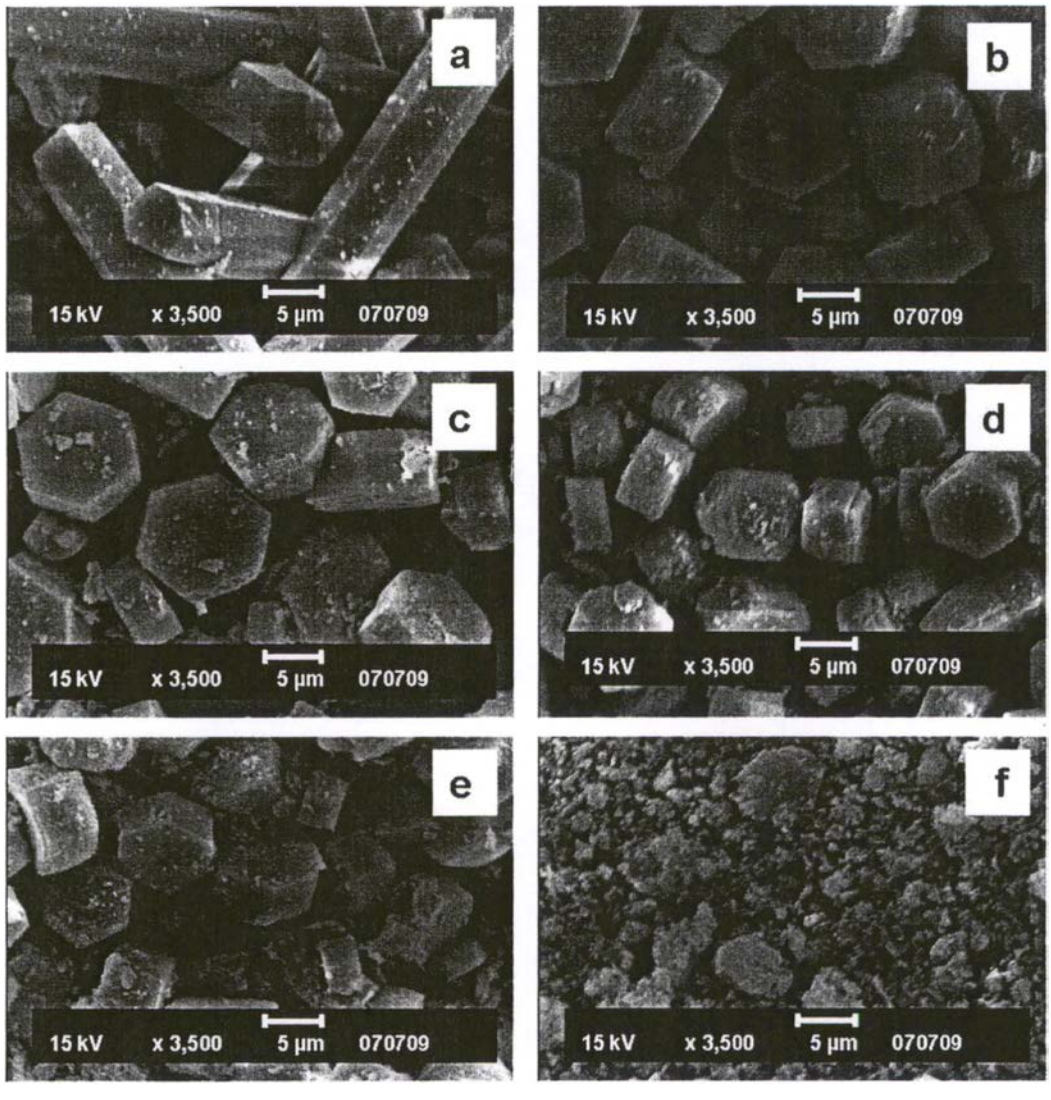

Figure 5.6 SEM images of SAPO-5 obtained from the mixture of Al_2O_3:$2P_2O_5$: $x$$SiO_2$:1.5TEA:750$H_2O$ at 190 °C for 1 h where x is the mole ratio of SiO_2/Al_2O_3 of (a) 0, (b) 0.2, (c) 0.4, (d) 0.6, (e) 0.8, and (f) 1.0.

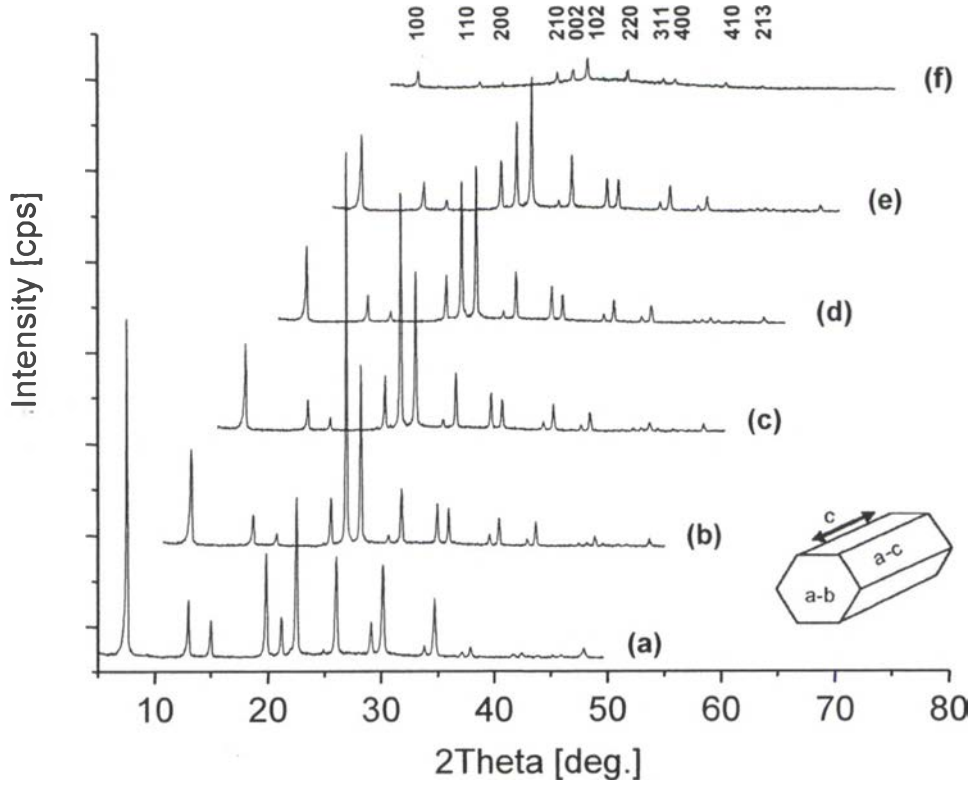

Figure 5.7 XRD patterns of SAPO-5 synthesized from the mixture of Al_2O_3:$2P_2O_5$: 1.5TEA:$x$$SiO_2$:750$H_2O$ at microwave temperature of 190 °C for 1 h where x is the mole ratio of SiO_2 to Al_2O_3 of (a) 0, (b) 0.2, (c) 0.4, (d) 0.6, (e) 0.8, and (f) 1.0.

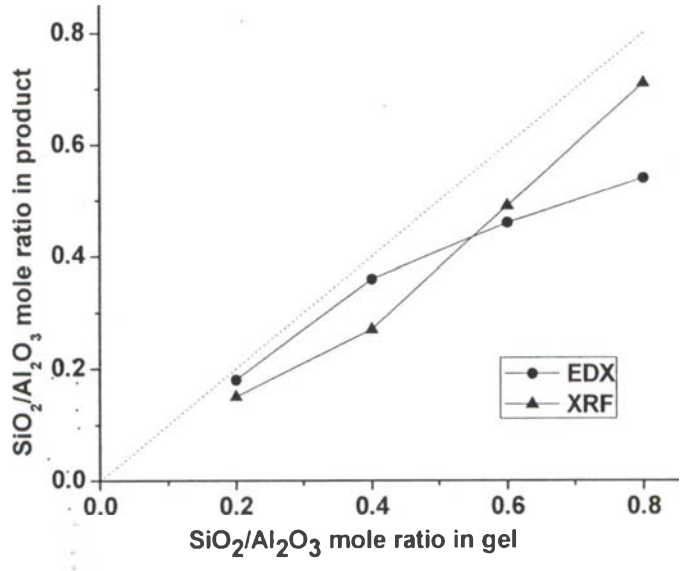

Figure 5.8 XRF and EDX/SEM results of the SiO_2 content in the reactant gels and the products synthesized from the mixture composition of Al_2O_3:$2P_2O_5$:$x$$SiO_2$:1.5TEA:750$H_2O$ at 190 °C for 1 h.

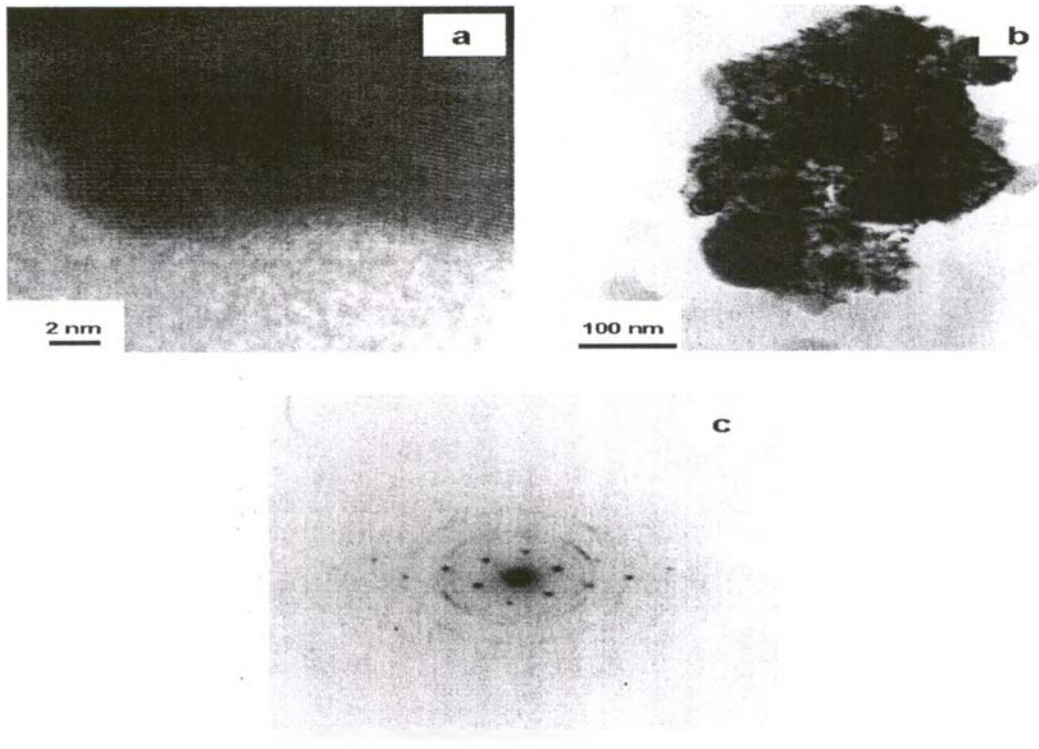

Figure 5.9 TEM results of SAPO-5synthesized from the mixture composition of Al_2O_3:$2P_2O_5$:$0.2SiO_2$:1.5TEA:$750H_2O$ at the reaction temperatures of 190 °C for 1 h; (a) hexagonal crystal, (b) nonstructural mesoporous, and (c) SAED of the nanostructure of mesoporous.

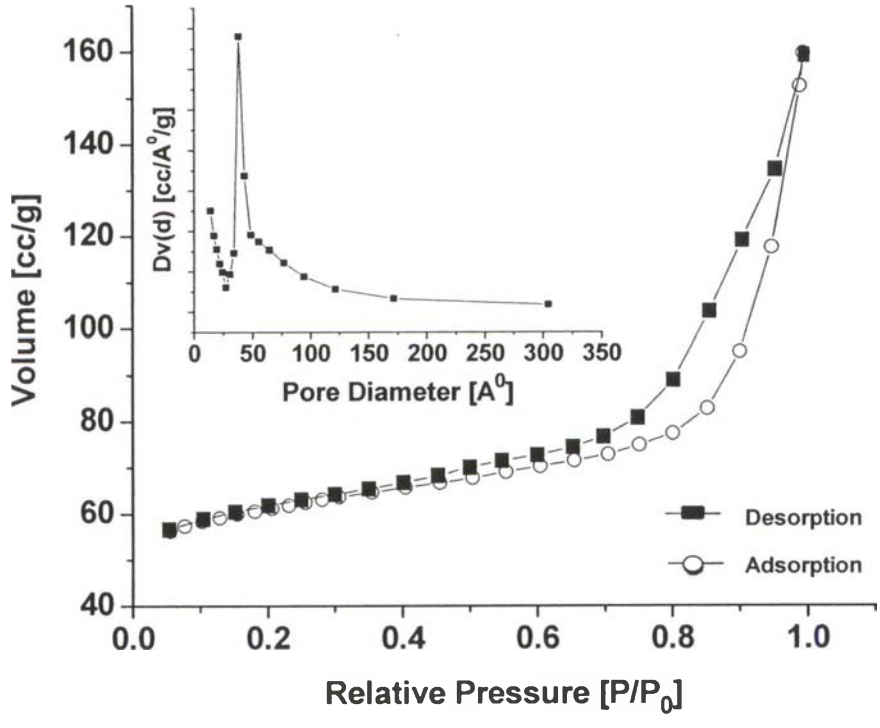

Figure 5.10 Nitrogen physisorption isotherm of SAPO-5 synthesized from the mixture composition of Al_2O_3:$2P_2O_5$:$0.2SiO_2$:1.5TEA:$750H_2O$ at the reaction temperatures of 190 °C for 1 h. Inset is corresponding pore size distribution.

Table 5.1 %Crystallinity of the SAPO-5, AFI products synthesized from the mixture of Al_2O_3:P_2O_5:1.5TEA:750H_2O at 190 °C for 1 h using different SiO_2/Al_2O_3 mole ratios.

SiO_2/Al_2O_3 mole ratio	**Crystallinity (%)[a]**
No SiO_2	99.72
0.2	100.00
0.4	78.45
0.6	62.90
0.8	54.36
1.0	17.64

[a] The 100% crystallinity of SAPO-5, AFI crystal was obtained from the sample synthesized using the same condition.

Table 5.2 Nitrogen physisorption data of the samples synthesized using different SiO_2/Al_2O_3 mole ratios at the reaction temperature of 190 °C for 1 h.

SiO_2/Al_2O_3 mole ratio	**V_{micro} (cm^3/g)[a]**	**V_{meso} (cm^3/g)[b]**	**BET area (m^2/g)[c]**
0.2	0.12	0.03	272
0.4	0.13	0.08	291
0.6	0.13	0.10	312
0.8	0.12	0.16	314

[a] Calculated by *t*-method Micro Pore Volume.

[b] Calculated by BJH method (desorption).

[c] Calculated by BET method.